| JMATPRO | Journal of Advanced Materials and Processing<br>12 (45): 3-14, Winter 2024<br>https://sanad.iau.ir/journal/jmatpro<br>Doi: 10.71670/jmatpro.2024.1217569 |
|---|---|

Research Paper

# Adsorption of Methyl Orange Dye from the Contaminated Water by Use of Sawdust Based Biosorbent: Effects of Different Precursors and Activation Methods

**Hadi Baseri[*1], Pooya Fazlali[2], Amir Hussein Hooshmand Poor[1]**

*1. Department of Materials Sciences & Engineering, School of Chemistry, Damghan University, Damghan Iran.*

*2. Joint Program Polymer Science Between Free University of Berlin, Humboldt university of Berlin, Technical University of Berlin and university of Potsdam, Berlin, Germany.*

**ARTICLE INFO**

*Article history:*

Received 11 September 2025
Revised: 22 November 2025
Accepted 11 December 2025
Available online 5 January 2024

*Keywords:*
*Biosorbent*
*Sawdust*
*Activation*
*methyl orange.*

**ABSTRACT**

The high concentrations of various industrial pollutants in atmospheric waters present a significant environmental challenge due to their widespread occurrence and high resistance to degradation. Therefore, the development of low-cost and eco-friendly methods, such as the production of new biosorbents, is essential. In this study, three commonly used types of sawdust—Walnut, Russian, and Forest wood—were utilized to produce different biosorbents for the removal of the anionic dye methyl orange from contaminated water. The effects of various physical and chemical activation methods on the adsorption capacity of these biosorbents were examined. The produced biosorbents were characterized using FTIR and SEM analyses, and the results were compared. Additionally, Langmuir, Freundlich, and Sips isotherms were employed for the isotherm studies. Based on the reported results, biosorbents with pore sizes of less than 1 µm and the highest adsorption capacities of approximately 800 mg/g were produced from all three types of sawdust studied after the pyrolysis process. However, a comparison between produced biosorbents show the samples derived from Russian sawdust exhibited relatively higher adsorption capacities of 80, 380, and 760 mg/g after solvent extraction, chemical activation, and pyrolysis processes. In addition, the maximum adsorption capacities were achieved in minimum adsorbent dose of 0.01 g per 100 ml of solution. Among all the studied isotherms, the Sips model, with $R^2$ values close to one, was found to be the best-fitting isotherm.

**Citation**: Baseri, H.; Fazlali, P.; Hooshmand Poor, A.H. (2024). Adsorption of Methyl Orange Dye from the Contaminated Water by Use of Sawdust Based Biosorbent: Effects of Different Precursors and Activation Methods, Journal of Advanced Materials and Processing, 12 (45), 3-14. Doi: 10.71670/jmatpro.2024.1217569



[*] **- Corresponding Author:**
E-Mail: baseri@du.ac.ir

## 1. Introduction

Sawdust is a significant byproduct of the wood industry, generated during the processing of timber into various products. In 2020, the global production of sawdust was approximately 38 billion tons [1], closely linked to the types of trees harvested, the volume of lumber produced, and the processing methods employed. Major sawdust-producing countries include the United States, Canada, Russia, and Brazil, which are also among the largest producers of timber. The production levels of sawdust in these countries reflect their extensive forestry resources and advanced wood processing industries [2, 3, 4].

Sawdust has a wide range of applications across various industries. In many countries, it is primarily used in the paper manufacturing process, where it serves as a raw material for producing wood pulp. Additionally, sawdust is utilized in the production of engineered wood products, such as particleboard and MDF (medium-density fiberboard) [5,6]. In Europe, sawdust is increasingly recognized as a renewable energy source, being used as biomass fuel in power plants for heating, electricity generation, and bioethanol production [7]. Furthermore, in construction, sawdust is often employed as an insulating material and in composite materials, enhancing structural integrity [8]. These diverse applications highlight the economic importance of sawdust and its role in sustainable practices worldwide.

Walnut wood, hardwoods (forest wood), and Russian wood (Siberian larch and pine) are some of the common types of wood used in Iran [9]. Consequently, their sawdust is readily available. In this study, the sawdust of these three commercially significant woods was selected as the precursor, and the effects of different activation methods on the adsorption capacities of the selected sawdust were investigated. The production of various biosorbents from sawdust and the adsorption of different contaminants from aqueous media have been reported in the literature [1, 10-13].

For example, Sadoun et al. (2023) [14] produced a high-performance biosorbent from Algerian Zean oak sawdust for removing methylene blue from aqueous solutions. Their batch experiments varied parameters such as contact time, particle size, pH, temperature, adsorbent dose, and initial dye concentration. They optimized these parameters, achieving an adsorption capacity of 52.376 mg/g. Naz et al. produced cobalt ferrite-functionalized sawdust for the adsorption of arsenite from aqueous solutions [11]. They created low-cost biosorbents from sawdust using different activation methods, including citric acid activation and steam activation, to enhance surface characteristics through the combined effects of activation and functionalization. Additionally, Zhao et al. [12] developed functionalized magnetic sawdust hydrochar for the elimination of tetracycline and demonstrated the influence of various operating parameters on the adsorption process. Different sawdust-based biosorbents reported in literature were reviewed by Castanon and his coworkers [15]. They show the produced adsorbents from sawdust of different woods have the wide adsorption capacities between 15 to 1500 mg/g for the adsorption of different heavy metal ions from the contaminated water. Furthermore, the relatively same results were reported by Sutherland and Chittoo [16].

In this study, three main types of sawdust available in Iran were selected, and three distinct processes—extraction of volatile and semi-volatile compounds, chemical activation, and thermal activation—were performed on them. Ultimately, the ability of the biosorbents to absorb methyl orange was examined. By comparing the biosorbents made from different precursors and evaluating the impact of various activation processes on their adsorption capacities, it can be determined which precursor is the most suitable for producing an effective biosorbent.

## 2. Materials and methods

### 2.1 Materials

Sawdust from Russian wood, walnut wood, and forest wood was obtained from a carpentry shop in Karaj, Iran. The sawdust was collected directly from sawmill waste and sieved using a sieve shaker with a 5 mm pore diameter. All chemicals used in this study were of analytical grade. Ethanol (96%) was obtained from Ghatran Shimi (Iran), while phosphoric acid ($H_3PO_4$, 85%) was purchased from Sigma-Aldrich. The solutions were prepared using double-distilled water, and nitrogen gas (99% purity) was purchased from Sabalan Gas Co. (Iran).

### 2.2 Production of biosorbent

The extractable components of the sawdust were separated using a Soxhlet extractor. In this process, 15 g of each sample was placed in a thimble and extracted with 250 mL of 96% ethanol in a Soxhlet extractor (ASEMANLAB, Iran) for approximately 24 hours. After the solvent extraction, the remaining sawdust was dried in an oven at 80°C for 12 hours.

For the chemical activation of the samples, the remaining sawdust from the extraction process was mixed with a phosphoric acid ($H_3PO_4$) solution (25 w%, 30°C, 24 h) under magnetic agitation. Subsequently, the mixture was neutralized by washing with distilled water, and then it was dehydrated in an oven overnight at 105°C.

Pyrolysis is the final step in the production of biosorbent. In this process, an electrical furnace (8

cm ID, 15 cm length, 500 W) capable of reaching temperatures up to 700°C (±5) was used in fixed bed mode. For the pyrolysis experiments, the desired weights of feedstock were charged into the furnace. The experiments were conducted in a closed system with a constant nitrogen ($N_2$) flow rate of 3 $cm^3/s$ and at a constant temperature of 500°C for 2 hours. At the end of the experiment, the system was allowed to cool down for three hours, after which the nitrogen gas flow was cut off and the furnace was opened. Finally, the residual biochar was collected in closed vessels for further experiments.

## 2.3 Analyses of the produced biosorbents

The organic structures and functional groups in the different produced biosorbents were analyzed using Fourier Transform Infrared (FTIR) spectroscopy with a Unicam 4600 FTIR spectrometer (Mattson, USA), scanning wave numbers from 400 to 4000 $cm^{-1}$. The morphology and shape of the particles on the surface of the produced biosorbents were examined using a Field-Emission Scanning Electron Microscope (FE-SEM) (TESCAN BRNO-MIRA3 LUM), operating at an accelerating voltage of 10 kV and a maximum magnification of 100 kX.

## 2.4 Adsorption Experiments

Batch mode adsorption experiments were conducted in this study. For each experiment, 0.02 g of the biosorbent was added to approximately 100 mL of the stock solution with the desired concentration in an Erlenmeyer flask. The system was agitated at 200 rpm using an electromagnetic heater stirrer at a constant temperature of 25°C for 1 hour. At the end of the adsorption experiment, the adsorbent particles were separated by centrifugation and filtration through filter paper, and the concentration of the remaining solution was determined using a UV/Vis spectrophotometer. The adsorption capacities $q_t$ (mg/g) of the biosorbents were calculated using Eq. 1.

$$q_t = \frac{(C_i - C_f)}{m} \times V \quad (1)$$

In which $C_i$ and $C_f$ are the initial and final concentrations of MO (mg/L) in the reminded solution, $V$ is the volume of solution (L), and $m$ is the mass of used biosorbent (g).

## 3. Results and descusion

## 3.1 SEM Analysis

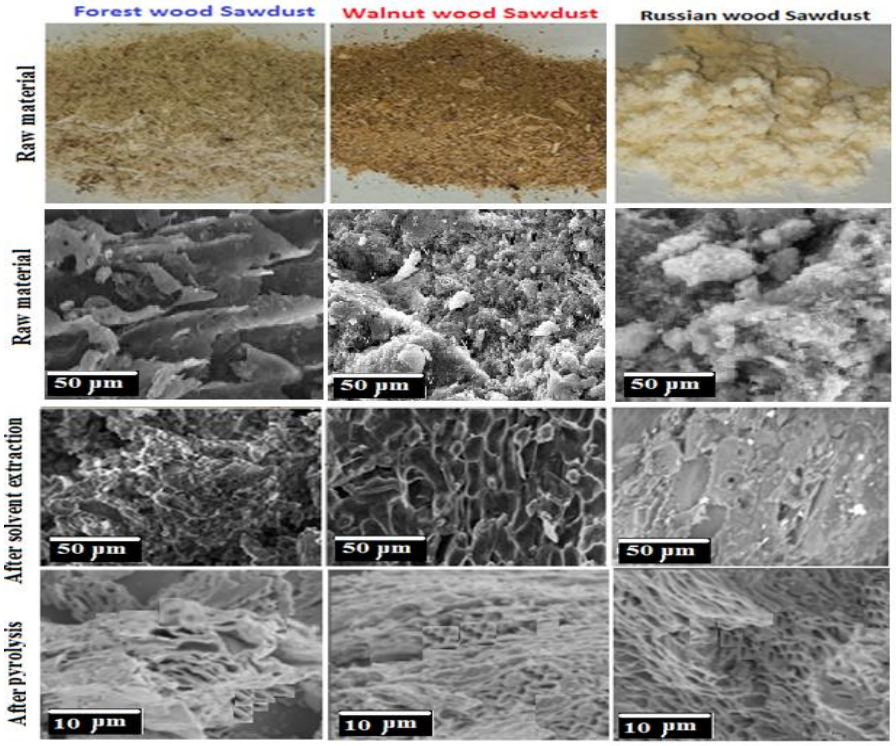


**Fig. 1.** The macroscopic and SEM images of the produced biosorbents from the different presursors of Forest wood sawdust, Russian wood sawdust, and Walnut wood sawdust

The SEM images of the produced biosorbents after solvent extraction and pyrolysis are depicted in Figure 1. As shown, after the solvent extraction process, the size of the pores on the surface of the different sawdust samples ranged from 1 to 10 µm. However, after the pyrolysis process, the size of the pores decreased to about 1 µm or less.

## 3.2. FTIR Analysis of the produced biosorbents

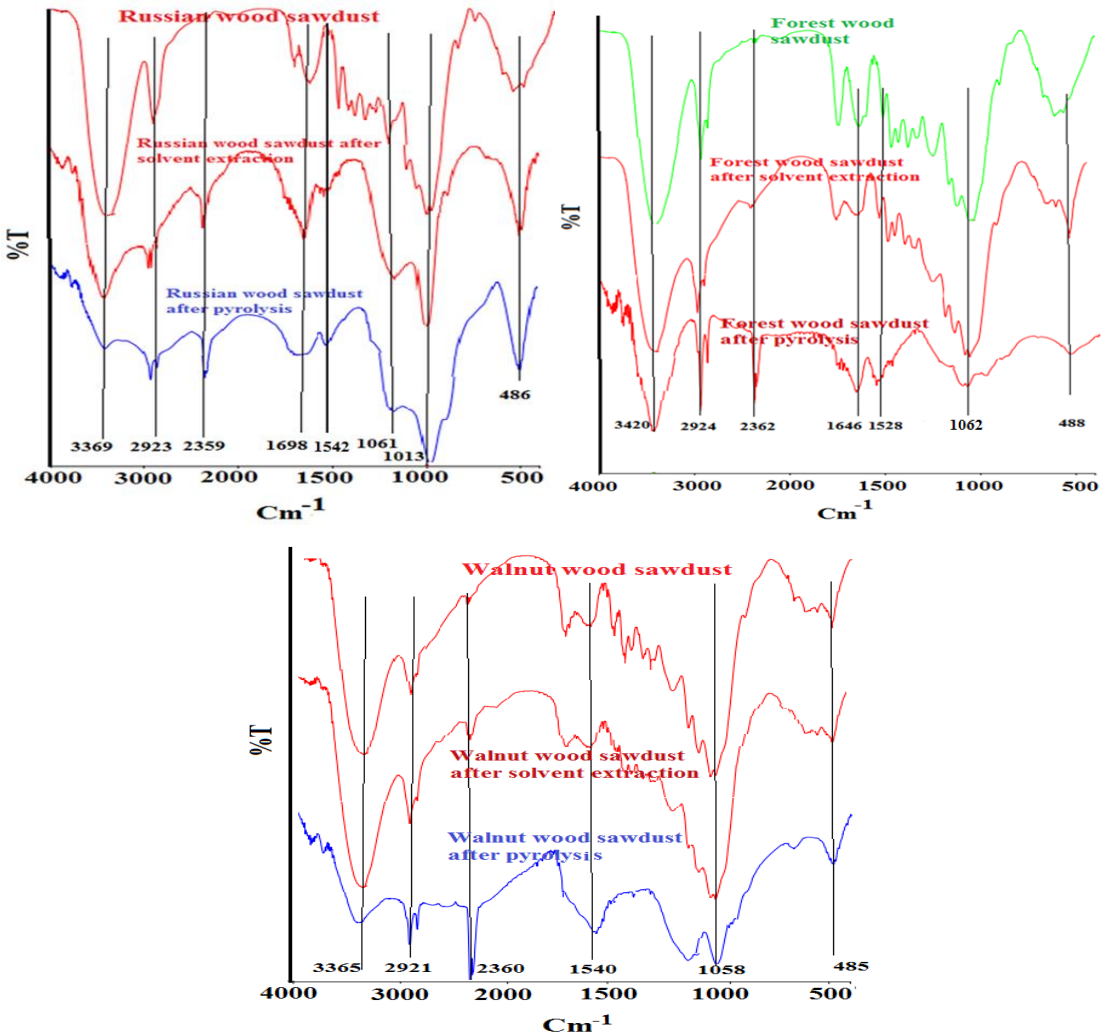


**Fig. 2.** FTIR spectra of the produced biosorbents from deferent precursors and by various activation methods.

Figure 2 shows the FTIR spectra of Russian, forest, and walnut wood sawdust before and after treatment with solvent extraction and pyrolysis processes. As expected, all the sawdust samples are primarily composed of cellulose, hemicellulose, and lignin, exhibiting the following main characteristic peaks:
The broad band at approximately 3200 to 3600 $cm^{-1}$ is associated with hydroxyl groups (OH) in the cellulose structure [17, 18]. Additionally, the C-H bands observed between 2800 and 3000 $cm^{-1}$ correspond to the methyl and methylene groups in hydrocarbons [19]. The bands in the range of 1050 to 1150 $cm^{-1}$ are attributed to the deformation, stretching, and bending vibrations of (C=O, C-O, and C-H) bonds in lignin molecules [20]. Furthermore, the peaks around 1510 to 1600 $cm^{-1}$ may be related to C=C skeletal bands in aromatics or the stretching or bending of C=C groups in lignins [21]. The carbonyl (C=O) and ether (C-O-C) groups in hemicellulose are likely responsible for the peaks observed at approximately 1730-1750 $cm^{-1}$ and 900-1200 $cm^{-1}$ [21, 22]. Finally, the bands at 914, 540, and 470 $cm^{-1}$ are attributed to Si-O-Si bending vibrations [19].

Based on the results reported in Figure 2, the concentration of O-H groups decreased significantly for all the studied samples after the pyrolysis experiments. This reduction is attributed to the significant decrease in water molecules, alcohols, phenols, and other O-H containing components during the pyrolysis process. The vibration peaks at approximately 2360 $cm^{-1}$ may be attributed to C=O bonds in $CO_2$ molecules. The intensity of these peaks increased after solvent extraction and, specifically, rose further after the pyrolysis process. Solvent extraction led to the removal of essential oils and the main components of other extractable molecules, thereby increasing the adsorption capacity of the samples. With the enhanced adsorption capacity, $CO_2$ molecules may adsorb more effectively on the surface of the samples, resulting in higher intensity of the related peaks. This phenomenon is observed more intensely after pyrolysis.
The main bands associated with groups related to lignin (aromatic or benzene rings) are observed in the signals within the range of 1510 $cm^{-1}$ to 1590 $cm^{-1}$ [23]. The increase in the intensity of these peaks after the solvent extraction and pyrolysis processes

indicates a higher concentration of the related chemicals following these treatment processes. This is due to the removal of more unstable and smaller molecules during these processes.

The band around 1060 $cm^{-1}$ is associated with C-O groups in primary alcohols, which decreased significantly during the pyrolysis process. Moreover, peaks related to phosphorus-containing compounds are generally detected in the range of 950 to 1200 $cm^{-1}$. As shown in Figure 2, a higher intensity of these peaks is observed after chemical activation. Finally, the metal oxide groups and the Si-O group exhibit an adsorption peak around 460 $cm^{-1}$. The relatively constant intensity of this peak across all studied samples indicates that the concentrations of Si-O and metal oxides did not change significantly during the various treatment processes.

### 3.3 The effects of activation method on the adsorption capacity of methyl orange

Activation is a crucial process in the production of biosorbents. Different activation methods significantly alter the adsorption capacity of biosorbents [24]. However, activation processes can be costly and contribute substantially to the final cost of the produced biosorbents. In this work, various physical and chemical activation methods were employed to produce different biosorbents from various precursors, including sawdust, and the adsorption capacities of the produced biosorbents are compared in Figure 3.

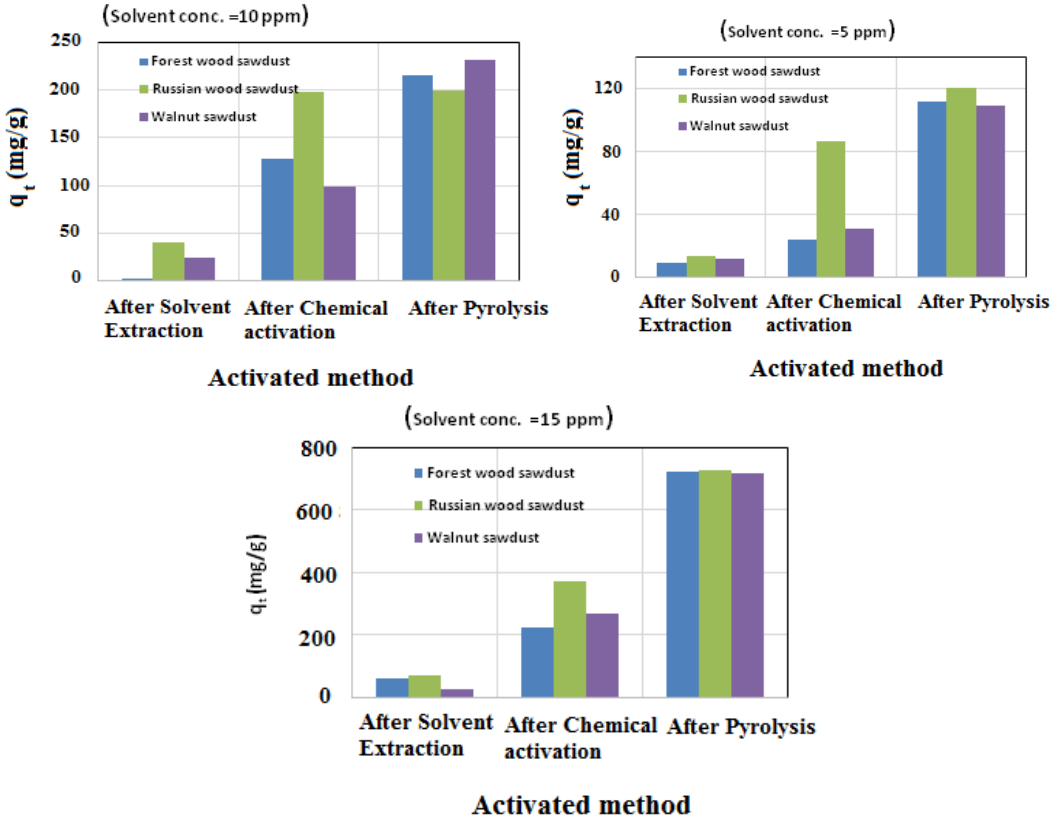


**Fig. 3.** The adsorption capacities of the different produced biosorbents from different precursors and activation methods.

In this figure, the adsorption capacity of raw sawdust is not reported because it is very low in comparison to the others. Additionally, the use of raw sawdust introduced some painting and oily components into the system.

Based on the results depicted in Figure 3, the adsorption capacities of all the studied sawdust samples after the solvent extraction process are below 100 mg/g. However, after chemical activation with phosphoric acid, the adsorption capacities of the samples increased several times, and they are reaching their maximum values after the pyrolysis process.

Through the solvent extraction process, relatively all extractable components, such as lipids and essential oils, are removed from the sawdust, leaving behind empty sites that can act as adsorption surfaces. Activation with phosphoric acid modifies the topological and textural properties of the biosorbent, resulting in a relatively large surface area [25]. Consequently, the dye component of methyl orange is better adsorbed onto the surface of the produced biosorbent.

During the chemical activation process, sawdust particles come into direct contact with phosphoric acid molecules. As a result, some of the mineral elements present within them, such as metals, dissolve into the acid.
Therefore, it strongly influenced the porous structure of resulting activated carbon. Additionally, some sites within the sawdust particles become activated upon contact with $PO_4^{-3}$ ions. The results presented by some researchers [26] also indicate that chemical activation with phosphoric acid can lead to an increased efficiency in the adsorption of anionic dyes such as methyl orange. However, considering the different sources of the sawdust used, this variation in adsorption capacity differs for the three types of studied sawdust.

Finally, as noted in the literature [27, 28], the pyrolysis process in a muffle furnace under a neutral atmosphere leads to higher adsorption capacities. Therefore, the best biosorbent with the highest adsorption capacity is produced after the pyrolysis process. A comparison between different precursors shows that Russian wood sawdust is relatively the best precursor for the production of biosorbents. However, after pyrolysis, all the produced biosorbents demonstrate relatively similar adsorption capacities for the adsorption of methyl orange dye.

### 3.4 The effects of dose of biosorbent on the adsorption capacity of methyl orange

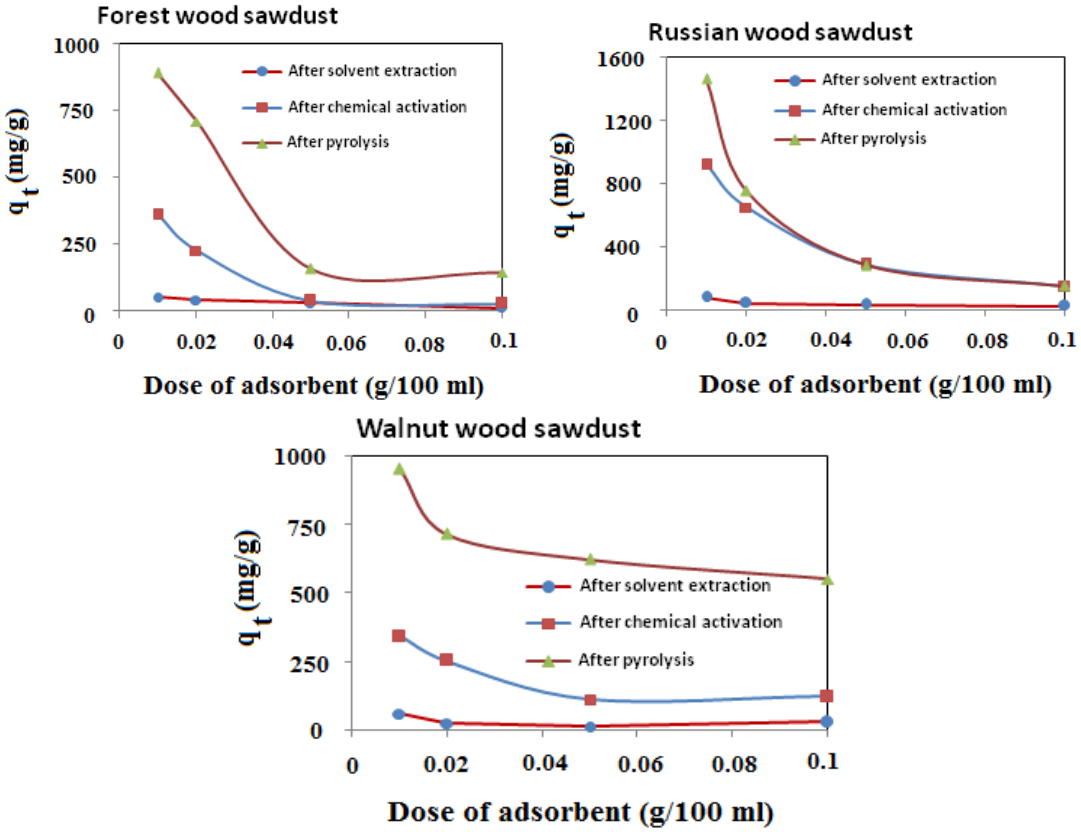


**Fig. 4.** The adsorption capacities of the different produced biosorbents in various doses of the used biosorbents.

Figure 4 shows the effects of biosorbent dosage on the adsorption capacity of the methyl orange dye at a solution concentration of 20 ppm. As illustrated, for the studied biosorbents with different precursors and activation methods, increasing the biosorbent dosage from 0.01 g to 0.1 g in 100 ml of solution resulted in a continuous decrease in adsorption capacity. However, the adsorption capacity remained relatively constant at biosorbent dosages greater than 0.05 g in 100 ml of the stock solution. By increasing the adsorbent dosages, oversaturation or coverage of active sites occurs, reducing the availability of binding sites for dye contaminants and therefore the adsorption capacity decreased slightly. However, this effect is diminished in adsorption capacities higher than 0.05 g per 100 ml of solution. Similar results have been reported in the literature regarding the adsorption of ciprofloxacin and methylene blue by biosorbents produced from various precursors, such as chitosan and the biomass of *Aptenia cordifolia* [29, 30].

### 3.5 The effects of solution concentration on the adsorption capacity of methyl orange

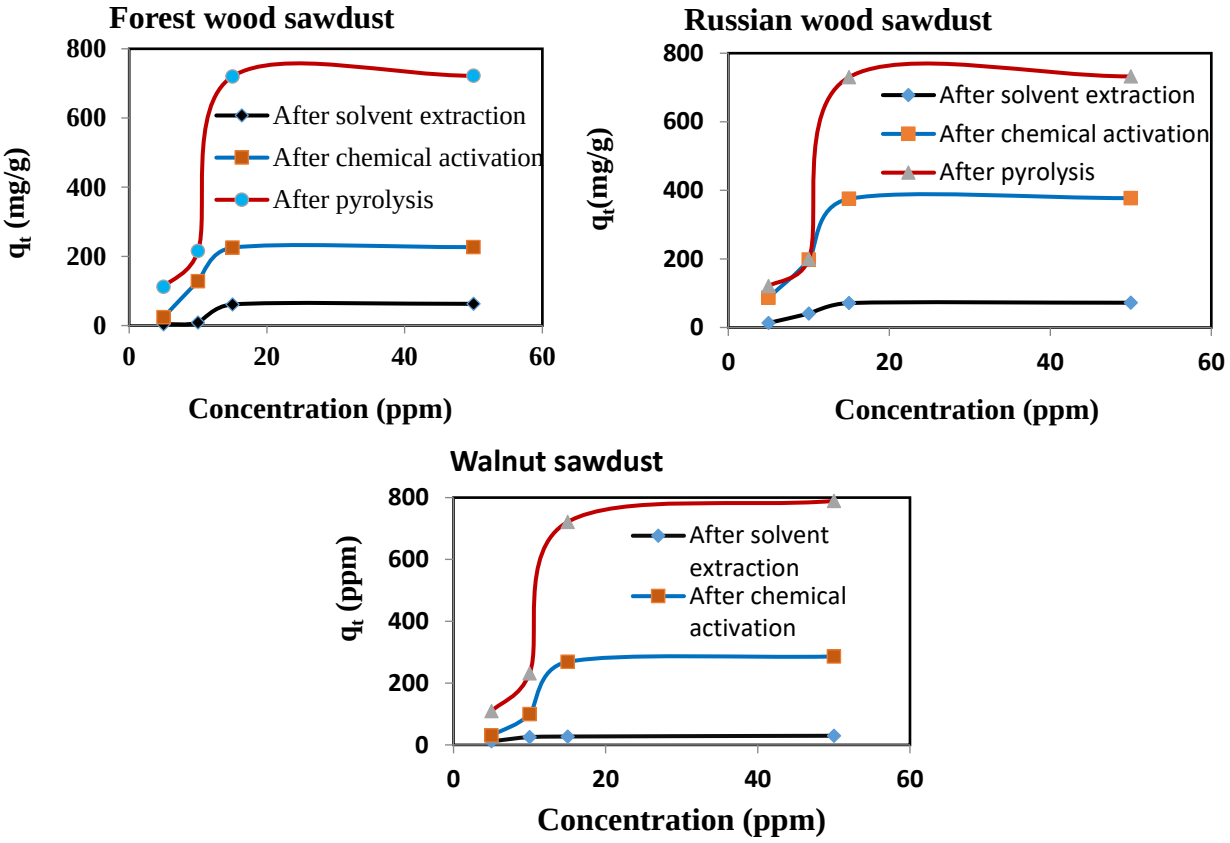


**Fig. 5.** The adsorption capacities of the different produced biosorbents in the various concentrations of solution.

The influence of the initial concentration of methyl orange (MO) on the adsorption capacity of the various produced biosorbents is illustrated in Figure 5. This was assessed by varying the solution concentration between 5 to 50 ppm while maintaining an adsorbent dosage of 0.2 g/L at neutral pH. As the solution concentration increased from 5 to 15 ppm, the adsorption capacity of all studied biosorbents increased. However, at higher solution concentrations, no significant increase in adsorption capacities was observed. This variation can be attributed to the enhancement of the driving force for mass transfer as the initial concentration rises, which promotes the biosorption of MO [31]. Beyond an initial concentration of 15 ppm, by increasing the dye concentration in 100 ml of solution, the active sites on the surface of the biosorbent may be saturated and this process is in competition with the increasing driving force of mass transfer and therefore the amount of dye removed stabilizes [32]. Consequently, the adsorption capacity reaches a plateau. Relatively the same results were reported by Zein et al [33] for the adsorption of methylene blue using solid waste of lemongrass biosorbent.

Figure 6 shows the effect of adsorption time on the adsorption capacity of the produced biosorbent from the Russian sawdust after chemical activation and pyrolysis processes. As observed, after 60 minutes of adsorption time, the adsorption capacities of the studied samples reached constant values.

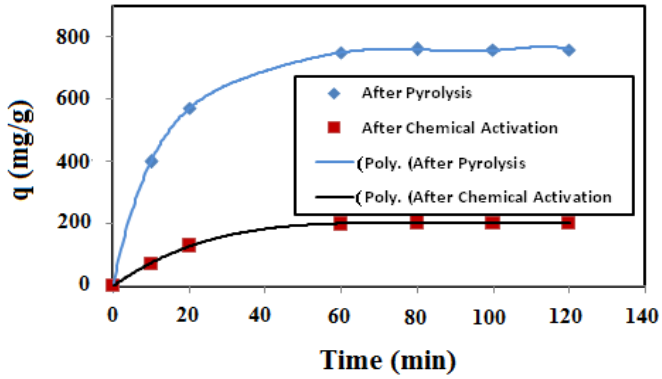


**Fig. 6.** Effect of adsorption time on the adsorption capacity of the biosorbents produced from the Russian sawdust after chemical activation and pyrolysis processes**.**

## 3.6 Adsorption mechanism

As mentioned in the literature [34], phosphoric acid molecules act as acidic catalysts in the activation process. They may facilitate the cleavage of bonds and the formation of crosslinks through dehydration processes, leading to the creation of micro- and mesopores in the resulting biosorbent. Furthermore, the organic components of biomass can interact with $H_3PO_4$ to form carbonaceous, polyphosphate, and phosphorus compounds. These compounds crosslink the biopolymer fragments derived from the lignocellulosic components of biomass, enhancing interactions with adsorbate molecules.

Additionally, the phosphate groups present in the biosorbent matrix contribute to the expansion of the structure, resulting in a porous configuration. This alteration in functional groups increases accessibility for the biosorption of organic pollutants. Therefore, chemical activation with $H_3PO_4$ can lead to significant modifications in morphology, surface area, and surface functional groups, which favorably influence interactions with various organic pollutants. Methyl orange is an anionic dye characterized by its aromatic rings in the chemical structure. The adsorption mechanisms of MO onto porous carbonaceous materials typically involve simultaneous interactions of varying natures. The nature of these interactions is influenced by several parameters, including the characteristics of the adsorbed contaminant and the properties of the adsorbent used.

In this study, the high porosity of the produced biosorbents and the presence of pores of varying sizes on their surfaces (as evidenced by the reported SEM images) facilitate the diffusion of MO molecules through the internal pore network via a pore-filling mechanism.

Furthermore, physical adsorption occurs through weak attractive forces, such as van der Waals forces, between the adsorbate molecules and the surface of the adsorbents. This phenomenon is primarily observed in adsorbents with micronized pores.

Another type of interaction to consider is that the MO molecule contains two aromatic rings in its structure, while the produced activated biosorbent exhibits a certain degree of graphitized structure. This allows for π-π interactions to occur, where the π-electrons (donors) of the activated biosorbent can interact with the π-electrons (acceptors) of the MO molecules.

Moreover, FTIR analysis indicated that the structure of the produced biosorbent contains functional groups with phosphorus and oxygen, a consequence of the $H_3PO_4$ treatment. These atoms, possessing non-bonding electrons, can interact with the aromatic structure of the MO molecule through n-π interactions.

Another type of interaction that may occur is hydrogen bonding. This can arise from interactions between the hydrogen atoms in polar functional groups present on the surface of the adsorbent, such as -OH and -COOH, and the nitrogen or oxygen atoms in the MO molecules.

## 3.7 Adsorption isotherm

Isotherm studies are used to understand the surface properties, adsorbent–adsorbate interactions, adsorption mechanisms, and adsorption capacity of the produced biosorbents. These studies describe the release or retention of a specific substance from the liquid phase to the solid phase of the adsorbent at a constant temperature [35].

**Table 1.** The isotherm parameters for the different used models

**Forest wood sawdust**

| | After solvent extraction | | | | After chemical activation | | | | After pyrolysis | | | |
|---|---|---|---|---|---|---|---|---|---|---|---|---|
| **Model type** | **K** | **$N_O$** | **m** | **$R^2$** | **K** | **$N_O$** | **m** | **$R^2$** | **K** | **$N_O$** | **m** | **$R^2$** |
| **Langmuir** | 0.03327 | 106.56 | ----- | 0.9886 | 0.07134 | 315.38 | ----- | 0.9656 | 0.0523 | 1066.88 | ----- | 0.9817 |
| **Freundlich** | 5.9517 | ----- | 1.6106 | 0.9819 | 46.097 | ----- | 2.3189 | 0.9552 | 109.97 | ----- | 1.996 | 0.9746 |
| **Sips** | $3.04*10^{-8}$ | 59.908 | 0.1420 | 0.9935 | $1.56*10^{-5}$ | 234.52 | 0.2026 | 0.9946 | 0.9996 | 729.23 | 0.134 | 0.9996 |

**Russian wood sawdust**

| | After solvent extraction | | | | After chemical activation | | | | After pyrolysis | | | |
|---|---|---|---|---|---|---|---|---|---|---|---|---|
| **Model type** | **K** | **$N_O$** | **m** | **$R^2$** | **K** | **$N_O$** | **m** | **$R^2$** | **K** | **$N_O$** | **m** | **$R^2$** |
| **Langmuir** | 0.07906 | 97.706 | ----- | 0.9689 | 0.08160 | 505.36 | ----- | 0.9715 | 0.0523 | 1066.88 | ----- | 0.9817 |
| **Freundlich** | 16.259 | ----- | 2.4793 | 0.9598 | 87.892 | ----- | 2.5412 | 0.9633 | 109.97 | ----- | 1.996 | 0.9746 |
| **Sips** | $5.37*10^{-4}$ | 75.366 | 0.2896 | 0.9917 | 0.00141 | 396.91 | 0.3309 | 0.9892 | $1.59*10^{-8}$ | 729.23 | 0.134 | 0.9996 |

**Walnut sawdust**

| | After solvent extraction | | | | After chemical activation | | | | After pyrolysis | | | |
|---|---|---|---|---|---|---|---|---|---|---|---|---|
| **Model type** | **K** | **$N_O$** | **m** | **$R^2$** | **K** | **$N_O$** | **m** | **$R^2$** | **K** | **$N_O$** | **m** | **$R^2$** |
| **Langmuir** | 0.16412 | 35.293 | ----- | 0.969 | 0.05455 | 396.37 | ----- | 0.9784 | 0.05360 | 1064.06 | ----- | 0.981 |
| **Freundlich** | 11.842 | ----- | 3.9702 | 0.960 | 42.428 | ----- | 2.0224 | 0.9699 | 112.863 | ----- | 2.01855 | 0.974 |
| **Sips** | 0.00437 | 29.208 | 0.3195 | 0.999 | $2.5*10^{-8}$ | 272.695 | 0.1354 | 0.9996 | $4.58*10^{-8}$ | 734.605 | 0.14172 | 0.999 |

In this work, three isotherm models -namely Langmuir, Freundlich, and Sips- were employed to obtain the best fit for the equilibrium adsorption curves. Detailed descriptions of the models used are reported in the literature [36]. The estimated constants and statistical parameters obtained from the three selected isotherm models are summarized in Table 1.

Based on the results presented in Table 1, a comparison of the reported $R^2$ values shows relatively good agreement between the experimental results and the calculated values of the three isotherm models ($R^2$ >0.95). However, for all studied biosorbents, the Sips model, which has three adjustable parameters, demonstrates the best fit with the experimental data ($R^2$ >0.99). This model combines the characteristics of the Langmuir and Freundlich isotherms for situations where both neighboring interactions and heterogeneous adsorption are present. Specifically, the Sips isotherm model is used to describe the adsorption process in nonlinear and inhomogeneous systems.

A comparison between the Langmuir and Freundlich isotherm models, both with two adjustable parameters, shows that the Langmuir model fits the experimental data relatively better. This indicates that the monolayer adsorption model governs the adsorption of methyl orange dye molecules on the surfaces of biosorbents produced from the sawdust of the three different studied woods.

The Langmuir isotherm assumes homogeneous adsorption, which occurs exclusively at specific, uniform sites. Once an adsorbate occupies a site, no further adsorption can take place at that site, resulting in a characteristic plateau on the adsorption curve. Additionally, the model hypothesizes that there are no lateral interactions or steric hindrances between the adsorbed molecules [37-39].

## 4. Conclusion

The production of various biosorbents from the sawdust of walnut wood, forest wood, and Russian wood using different physical and chemical activation methods was studied in this work. A comparison between the adsorption capacities of produced biosorbents and other related works were reported in table 2. The results indicated that the biosorbents derived from Russian sawdust exhibited the highest adsorption capacity for methyl orange compared to the others. However, after the pyrolysis process, biosorbents produced from all studied sawdust types demonstrated relatively good performance for the removal of methyl orange from aqueous solutions. Based on the reported $R^2$ values, the Sips isotherm model, which has three adjustable parameters, shows the best fit, with an $R^2$ value close to one. Furthermore, when comparing two-parameter models, the Langmuir isotherm fits the experimental adsorption data better than the Freundlich model. Therefore, homogeneous monolayer adsorption is the dominant process for these systems.

**Table 2**. Comparison between biosorbents produced in this work and other related works.

| | feedstock | Modification method | Target adsorbed | q (mg/g) | References |
|---|---|---|---|---|---|
| **1** | Pine wood Sawdust | Chemical activation with Maleic acid | Cd (II) | 1804 | [40] |
| **2** | wood Sawdust | Chemical activation with $HNO_3$ & NaOH | Hg (II) | 528 | [41] |
| **3** | Commercial Sawdust | Boiling in distilled water Dried at 60°C | Methylene blue | 76.9 | [42] |
| **4** | barley straw | Washing with water and drying at 100°C | $Cu^{2+}$ and $Pb^{2+}$ | 4.6 , 23.2 | [43] |
| **6** | Rice straw | Chemical activation with KOH and NaOH | Methylene blue | 588, 232 | [44] |
| **7** | Russian Wood Sawdust | Solvent Extraction | Methyl Orange | 80 | This work |
| **8** | Russian Wood Sawdust | Solvent Extraction and $H_3PO_4$ Chemical activation | Methyl Orange | 380 | This work |
| **9** | Russian Wood Sawdust | Solvent Extraction, Chemical activation, and Pyrolysis at 500°C | Methyl Orange | 760 | This work |

**Author contribution** P. Fazlali and H. Baseri planed the work; P. Fazlali and A.H. Hoshmandpoor performed the experiments; H. Baseri analyzed the data and wrote the manuscript.

**Data Availability** Not applicable.

**Funding** Not applicable.

## Declarations

**Ethical approval** Not applicable.

**Competing interests** The authors declare no competing interests.

## References

[1] G. Zhou, S. Li, Q. Meng, C. Niu, X. Zhang, Q. Wang, A new type of highly efficient fir sawdust-based super adsorbent: Remove cationic dyes from wastewater. Surf Interfaces, 36 (2023) 102637.
[2] P. Stachowicz, M.J. Stolarski, Short rotation woody crops and forest biomass sawdust mixture pellet quality. Industrial Crops and Products, 197 (2023) 116604.
[3] A. Mwango, C. Kambole, Engineering Characteristics and Potential Increased Utilisation of Sawdust Composites in Construction—A Review. Journal of Building Construction and Planning Research, 7 (2019) 59.
[4] A. El Hamri A, Y. Mouhib, A. Ourmiche, M. Chigr, N.E. El Mansouri, Study of the Effect of Cedar Sawdust Content on Physical and Mechanical Properties of Cement Boards. molecules, 29 (2024) 4399.
[5] G.M. Ispas, I. Crăciunescu, S.C. Tripon, M. Dan, R.P. Turcu, Innovative oil removal system from water using magnetic nanocluster functionalized sawdust. Journal of Environmental Chemical Engineering, 13 (2025) 118558.
[6] H. aliyari, M. Shamsian, B. Nosrati, physical and mechanical properties of wood-plastic based on MDF sawdust with the addition of sawdust coal, sulfur and recycled rubber powder. Iranian Journal of Wood and Paper Industries, 14 (2024) 339.
[7] H.U. Ghani, H. Ilvesniemi, I. Leinonen, K. Ruuttunen, M.d. Musharof Hussain Khan, P. Oinas, P. Anttila, Evaluating sawdust-based bioethanol and pyrolysis products in the European Union: Feedstock availability, life cycle assessment, and techno-economic analysis. Environmental Impact Assessment Review, 115 (2025) 108035.
[8] E. Priya, P. Vasanthi, B. Prabhu, P. Murugesan, Sawdust as a sustainable additive: Comparative insights into its role in concrete and brick applications, Cleaner Waste Systems, 11 (2025) 100286.
[9] R. Oladi, S. Omidvari, K. Pourtahmasi, D. Efhamisisi D, Identification and verification of imported timbers in wood market of Iran; Part two: softwoods. J. of Wood and Forest Science and Technology, 28 (2021) 21.
[10] S. Naz, S. Alam, K. Rehan, S. Sultana, Adsorptive removal of new methylene blue from water by treated Malus domestica sawdust as a low cost biosorbent – equilibrium, kinetics and thermodynamic studies. Desalination and Water Treatment, 166 (2019) 72.
[11] H. Naz, Z. Khalid, S. Arif, A. Sattar, M.N. Ahmed, M. Waseem, High removal efficiency of arsenite from aqueous solution by cobalt ferrite functionalized sawdust driven activated carbon. Inorganic Chemistry Communications, 178 (2025) 114615.
[12] Y. Zhao, Y. Zheng, S. Lei, X. Jiang, Y. Zhang, J. Zhao, Q. Jiang, Y. Zhong, T. Chen, J. Gao, MOFs functionalized magnetic sawdust hydrochar for effective tetracycline elimination: Inherent roles of adsorption and mechanisms. Separation and Purification Technology, 378 (2025) 134534.
[13] A. Hashem, C.O. Aniagor, S. Farag, M. Fikry, A.A. Aly, A. Amr, Evaluation of the adsorption capacity of surfactant-modified biomass in an aqueous acid blue 193 system, Waste Management Bulletin, 2 (2024) 172-183.
[14] L. Sadoun, K. Seffah, A. Benmounah, A. Zerizer, D. Ghernaout, High-performance raw biosorbent derived from Algerian Zean oak sawdust for removing methylene blue from aqueous environments. Desalination and Water Treatmentment, 294 (2023) 233.
[15] L.A. Torres-Castanon, A. Robledo-Peralta, C. Antileo, F. de J. Silerio-Vazquez, J. B. Proal-Najera, Sawdust-based adsorbents for water treatment:an assessment of their potential and challenges in heavy metal adsorption, Journal of Hazardous Materials Advances, 18 (2025) 100758.
[16] C. Sutherland, B. Chittoo, Recent Devepolments in the Applicatio of Sawdust as a Biosorbent for Heavy Methal Cations: A Mini-Reviw, Materials International, 6(1) (2024) 1-15.
[17] A.W. Suciyati, P. Manurung, S. Sembiring, R. Situmeang, Comparative study of Cladophora sp. cellulose by using FTIR and XRD. Journal of Physics: Conference Series, 1751 (2021) 012075.
[18] S. Cichosz, A. Masek, K. Dems-Rudnicka, Original study on mathematical models for analysis of cellulose water content from absorbance/wavenumber shifts in ATR FT-IR spectrum. Scientific Reports, 12 (2022) 19739.
[19] V. Hospodarova, E. Singovszka, N. Stevulova, Characterization of Cellulosic Fibers by FTIR Spectroscopy for Their Further Implementation to Building Materials. American Journal of Analytical Chemistry, 9 (2018) 303.
[20] *E.A. Varol, U. Mutlu, Samples Based on the Thermal Decomposition Behavior of Hemicellulose. Energies, 16 (2023)* 3674.
[21] R. Javier-Astete, J. Jimenez-Davalos, G. Zolla, K. Schum. and G. crinita Lam. Determination of hemicellulose, cellulose, holocellulose and lignin content using FTIR in Calycophyllum spruceanum (Benth.), PLoS ONE, 16 (2021) e0256559.
[22] G. Ezequiel, Maderas. Fourier transform infrared spectroscopy in treated woods deteriorated by a white rot fungus. Ciencia y tecnología, 20 (2018) 479.
[23] R. Herrera, E. Hermoso, J. Labidi, J.I. Fernandez-Golfin, Non-destructive determination of

core-transition-outer wood of Pinus nigra combining FTIR spectroscopy and prediction models. Microchemical Journal, 179 (2022) 107532.
[24] J. LS Duarte, A. Hayat, C. M. Domínguez, A. Santos, S. Cotillas, Forest biomass derived biochar for effective meropenem mitigation in hospital effluents. Journal of Hazardous Materials Advances, 19 (2025) 100811.
[25] W.A. Khanday, M.J. Ahmed, P.U. Okoye, E.H. Hummadi, Single-step $H_3PO_4$ activation of chitosan for efficient adsorption of amoxicillin and doxycycline antibiotic pollutants. Inorganic Chemistry Communications, 175 (2025) 114189.
[26] A. Machrouhia , M. Farnanea , H. Tounsadib , Y. Kadmic, L. Favierd, S. Qourzale, M. Abdennouria, N. Barka, Activated carbon from Thapsia transtagana stems: central composite design (CCD) optimization of the preparation conditions and efficient dyes removal, Desalination and Water Treatment, 166 (2019) 259–278.
[27] S. Paşa, N. Yılmaz, Í. Bulduk, O, Alagöz, Effective adsorption performance of hemp root-derived activated carbon for tamoxifen-contaminated wastewater, Journal of Molecular Liquids 425 (2025) 127219.
[28] S. Mishra, M.K., Adsorptive removal of diclofenac on nanoporous anoxic sewage sludge biochar: Investigating the influence of carbonization temperature, Separation and Purification Technology, 354 (2025) 129322.
[29] Y. Gherraby, Y. Rachdi, M. El Alouani, B. Aouan, R. Bassam, R. Cherouaki, H. Saufi, E.h. Khouya, S. Belaaouad, Application of Aptenia cordifolia powder as a biosorbent for methylene blue retention from an aqueous medium: Isotherm, kinetic, and thermodynamic investigations, Desalination and Water Treatment, 318 (2024) 1 00263.
[30] E.B. Vamsi, M. Reshma, C.P. Devatha, Adsorption of ciprofloxacin antibiotic using chitosan graphene oxide hybrid beads, Case Studies in Chemical and Environmental Engineering, 10 (2024) 100982.
[31] A.H. Jawad, A.S. Abdulhameed, Mesoporous Iraqi red kaolin clay as an efficient adsorbent for methylene blue dye: adsorption kinetic, isotherm and mechanism study. Surf Interfaces Mar., 18 (2020) 100422.
[32] S. Rahmani, B. Zeynizadeh, S. Karami, Removal of cationic methylene blue dye using magnetic and anionic-cationic modified montmorillonite: kinetic, isotherm and thermodynamic studies. Appl Clay Sci 184 (2020) 105391.
[33] R. Zein, J.S. Purnomo, P. Ramadhani, Safni, M.F. Alif, C.N. Putri, Enhancing sorption capacity of methylene blue dye using solid waste of lemongrass biosorbent by modification method, Arabian Journal of Chemistry, 16(2) (2023) 104480.
[34] L.A. da Silva Ries, J.H. da Silveira Chies, L. de Mattos Soares, E.V. Benvenutti, F.P. Gasparin, Investigation of the Adsorption Capacity of H3PO4-Activated Biochar from Eucalyptus Harvest Waste for the Efficient Rrmoval of Paracetamol in water, Water, 17(17) (2025) 2654.
[35] K. Li, X. Chen, M. Chen, J. Zhang, X. Qin, K. Li, F. Wan, J. Fang, P. Ning, C. Zhang, High-performance MgO-CaO/C for $H_2S$ oxidation prepared by a facile co-pyrolysis of magnesium gluconate and $CaCO_3$, Separation and Purification Technology, 328 (2024) 125075.
[36] R. Nitzsche, R. Gröngröft, M. Kraume, Separation of lignin from beech wood hydrolysate using polymeric resins and zeolites-determination and application of adsorption isotherms, Separation and Purification Technology, 209 (31) (2019) 491.
[37] F. Gimbert, N. Morin-Crini, F. Renault, P.M. Badot, G. Crini, Adsorption isotherm models for dye removal by cationized starch-based material in a single component system: Error analysis, J. Hazard Mater, 157 (2008) 34.
[38] K.Y. Foo, B.H. Hameed, Insights into the modeling of adsorption isotherm systems, Chemical Engineering Journal, 156 (2010) 2.
[39] I. Langmuir, THE CONSTITUTION AND FUNDAMENTAL PROPERTIES OF SOLIDS AND LIQUIDS, Journal of American Chemical Society, 38 (1916) 2221.
[40] A. Hashem, S.M. Badawy, S. Farag, L.A. Mohamed, A.J. Fletcher, G.M. Taha Non-linear adsorption characteristics of modified pine wood sawdust optimised for adsorption of Cd(II) from aqueous systems, J. Environ. Chem. Eng., 8 (4) (2020), Article 103966,
[41] F.Z. Bouzid, A. Driouch, H. Aguedal, A. Aziz, A. Iddou, A. Bentouami, A. Thakur, G. Goel, M.E. A. Elaissaoui Elmeliani, Activated sawdust as a sustainable solution for mercury removal in contaminated waters, React. Kinet. Mech. Catal., 137 (4) (2024), pp. 2309-2330,
[42] Markandeya, A. Singh, S.P. Shukla, D. Mohan, N.B. Singh, D.S. Bhargava, R. Shukla, G. Pondey, V.P. Yadav, G.C. Kisku, Adsorptive capacity of sawdust for the adsorption of MB dye and designing of twe-stage batch adsorber, Cagent Environmental Science, (2015) 1:10758556.
[43] Erol Pehlivan, Türkan Altun, Serife Parlayıcı, Utilization of barley straws as biosorbents for $Cu^{2+}$ and $Pb^{2+}$ ions, Journal of Hazardous Materials 164 (2009) 982–986.
[44] M.J. Saad, M.S. Shajab, W.N.W. Bush, S.Misran, S.Zakaria, S. Xian Chin, C.Hua Chia, Comparative Adsorption Mechanism of Rice Straw

Activated Carbon Activated with NaOH and KOH,
Sains Malaysiana 49(11)(2020): 2721-2734.